The Astrophysical Journal, 820:141 (9pp), 2016 April 1 doi:10.3847/0004-637X/820/2/141

ELECTRON IRRADIATION AND THERMAL PROCESSING OF MIXED-ICES OF POTENTIAL RELEVANCE TO JUPITER TROJAN ASTEROIDS

Ahmed Mahjoub[1,2], Michael J. Poston[1,2], Kevin P. Hand[1], Michael E. Brown[2], Robert Hodyss[1], Jordana Blacksberg[1], John M. Eiler[2], Robert W. Carlson[1], Bethany L. Ehlmann[1,2], and Mathieu Choukroun[1]
[1] Jet Propulsion Laboratory, California Institute of Technology, Pasadena, CA 91109, USA; Mahjoub.Ahmed@jpl.nasa.gov
[2] California Institute of Technology, Division of Geological and Planetary Sciences, Pasadena, CA 91125, USA
Received 2015 November 23; accepted 2016 February 16; published 2016 March 30

ABSTRACT

In this work we explore the chemistry that occurs during the irradiation of ice mixtures on planetary surfaces, with the goal of linking the presence of specific chemical compounds to their formation locations in the solar system and subsequent processing by later migration inward. We focus on the outer solar system and the chemical differences for ice mixtures inside and outside the stability line for H_2S. We perform a set of experiments to explore the hypothesis advanced by Wong & Brown that links the color bimodality in Jupiter's Trojans to the presence of H_2S in the surface of their precursors. Non-thermal (10 keV electron irradiation) and thermally driven chemistry of CH_3OH–NH_3–H_2O ("without H_2S") and H_2S–CH_3OH–NH_3–H_2O ("with H_2S") ices were examined. Mid-IR analyses of ice and mass spectrometry monitoring of the volatiles released during heating show a rich chemistry in both of the ice mixtures. The "with H_2S" mixture experiment shows a rapid consumption of H_2S molecules and production of OCS molecules after a few hours of irradiation. The heating of the irradiated "with H_2S" mixture to temperatures above 120 K leads to the appearance of new infrared bands that we provisionally assign to $SO_2$and CS. We show that radiolysis products are stable under the temperature and irradiation conditions of Jupiter Trojan asteroids. This makes them suitable target molecules for potential future missions as well as telescope observations with a high signal-to-noise ratio. We also suggest the consideration of sulfur chemistry in the theoretical modeling aimed at understanding the chemical composition of Trojans and KOBs.

Key words: astrochemistry – Kuiper Belt: general – methods: laboratory: molecular – molecular processes – techniques: spectroscopic

1. INTRODUCTION

Jupiter Trojan asteroids are a population of small bodies captured around the L4 and L5 Lagrangian points of the Sun-Jupiter system. We currently know of over 6000 Jupiter Trojans with diameters ranging from 200 km to less than 1 km. The population among this family of asteroids can be categorized into two classes according to their visible (Szabó et al. 2007; Melita et al. 2008; Roig et al. 2008) and near-infrared (NIR) (Emery et al. 2011) spectra: red Trojans and less-red Trojans. The issue of how objects belonging to the same dynamical group have such diversity in their Vis-NIR spectra is tentatively linked to their origins and subsequent evolutions. While the origin of the Trojan Asteroids is not definitively known and is still a subject of research, dynamical models indicate that the Trojans may have been formed in the primordial Kuiper Belt region in the early solar system and were later captured into their present position (Morbidelli et al. 2005; Nesvorný et al. 2013). The hypothesis of multiple source regions has been suggested to explain the diversity of colors within the Jupiter Trojan population, i.e., the bimodality in color reflects the fact that this population is a mixture of bodies with two different origins (Emery et al. 2011; Marchis et al. 2012). Support for the hypothesis that the red and less-red Trojans formed in two different locations is given by Wong et al. (2014), where the two color populations were shown to have distinct magnitude distributions. The causes of the color differences remain undetermined, and thus further compositional information on the Trojan populations is needed to constrain where each of these populations originated. Laboratory experiments such as the ones we present here can guide observational studies of the Trojan asteroids by proposing chemical and compositional links between the formation location, subsequent evolution, and spectral properties of these bodies, linking specific chemical compounds to formation and processing conditions and specific spectral properties.

In addition to hypothesizing a link between the bimodal color of the Jupiter Trojans and their formation locations, Emery et al. (2011) argued that surface alteration (weathering and resurfacing) cannot alone explain the observed bimodality. Space weathering, driven by irradiation from energetic particles and photons, is believed to be responsible for the growth of organic-bearing refractory mantles covering the surfaces of icy, airless objects. The idea is that irradiation of organic ices drives a complex chemistry, leading to the production of a red crust. The bimodality in color would then be a result of differing ice compositions between the two populations. The chemistry leading to these two populations is far from being fully understood and needs to be studied by laboratory simulation experiments. As a first step in understanding this chemistry we address here the influence of including H_2S in the irradiation chemistry of carbon- and nitrogen- containing ices. The surface chemical composition of objects in the primordial planetesimal disk between 15 and 35 au is expected to be dependent on their orbital distance as well as their size. Wong & Brown (2015, submitted) suggest that a H_2S sublimation line located within the primordial trans-Neptunian disk divided objects in this region into two classes: sulfurous and sulfurless. This sharp change in the surface composition of the common progenitor of both Trojans and KBO's, followed by UV and particle irradiation, would lead to the surface color bimodality seen today in these two populations. In this hypothesis, the authors interpret the red and less-red Jupiter Trojans as descendants of

the sulfurous and sulfurless primordial trans-Neptunian objects that experienced heating and irradiation during their migration. If Trojans underwent migration during their history, understanding the different responses of different assemblages of compositionally diverse ices is critical. In particular, studying how S-bearing phases may bear on the spectral and chemical properties of ices is of major importance and critical test of this new hypothesis concerning Jupiter Trojans' colors. While some experiments (Thompson et al. 1987; Brunetto et al. 2006) show that the irradiation of carbon and nitrogen containing molecules leads to a reddening of the initial ice, no laboratory studies have tested whether the addition of sulfur containing molecules has an effect on the occurrence or magnitude of the observed reddening at relevant temperatures. The main goal of the present work is to investigate the chemical alterations that can occur on the icy surface of an object that is submitted to electron irradiation and heat in a migration processes from the primordial trans-Neptunian disk to Jupiter's L4 and L5 current points. Laboratory simulation of such processes is an explicit test of migration theories and helps constrain models of solar system formation and dynamical evolution. By submitting an ice analog to electron irradiation and subsequent heat, we study the resulting chemistry and spectral properties. In this work, ice chemistry in the "without H_2S" (CH_3OH–NH_3–H_2O) and "with H_2S" (H_2S–CH_3OH–NH_3–H_2O) mixtures was characterized by mid-IR spectroscopy and mass spectrometry. To the best of our knowledge the present study is the first reported work dealing with electron irradiation and heating of ice mixtures containing S, C, O, and N atoms.

This paper is structured as follows. In Section 2 we describe the experimental procedure. Our results are presented in Section 3. The astrophysical implications of this research are discussed in Section 4.

2. EXPERIMENTAL METHODOLOGY

Electron irradiation experiments were carried out using the Icy World Simulation Laboratory at the Jet Propulsion Laboratory. A detailed description of the facilities and capabilities of this laboratory can be found in Hand & Carlson (2011). The experimental setup consisted of a high vacuum stainless steel chamber pumped by a Varian Turbo and backed by oil-free pumps (base pressure $\sim 1 \times 10^{-8}$ torr). The ices were grown on a gold-coated glass substrate attached to the cold finger of a closed-cycle helium cryostat (ARS model DE-204). An external manifold was used to prepare gas mixtures prior to deposition. The ice film was grown by leaking the gas mixture into the chamber, forming ices on a gold mirror, which was held at 50 K. Most of the gas deposited directly, but a small fraction did not, resulting in a rise of chamber pressure of a few 10^{-8} torr. An electron gun was mounted on the chamber perpendicular to the substrate. High-energy electrons (10 keV) were directed at the ice with a typical beam current of 0.5 μA. A Faraday cup on a rotational stage was periodically placed between the electron gun and the ice film to monitor the electron beam current. All studied ices were submitted to the same fluence of electron energy $\sim 2 \times 10^{21}$ eV cm^{-2}. The fluence was estimated using

$$\text{Fluence} = E \times t \times \text{Flux}, \quad (1)$$

where E is electron energy, 10 keV, t is the irradiation time, and Flux is the number of electrons incident on the sample per unit area per second.

After irradiation for 19 hr, samples were warmed to 120 K at 0.5 K minute^{-1} while continuing electron irradiation. Samples were then irradiated an additional 1 hr at 120 K, the electron beam was turned off, and then the samples were warmed at 0.5 K minute^{-1} to room temperature. This experimental procedure was chosen to simulate the irradiation and heating history of an icy surface scattered from the primordial Kuiper Belt region (50 K) to Jupiter's Trojans' region (120 K). The chemical evolution of the ice was monitored with a Midac Fourier transform infrared spectrometer covering a wavenumber range 400–7000 cm^{-1} at 2 cm^{-1} resolution with 1024 scans accumulation. The angle of incidence of the infrared beam was $\sim 16^\circ$ to the normal of the ice film. The ice film was not optically thick: infrared light passed through the ice film and was reflected back through the film by the gold mirror to the detector where the intensity measured was divided by the intensity of reflected light from the gold mirror alone. A quadrupole mass spectrometer was used also to monitor the gaseous species released when the irradiated ices were warmed. This mass spectrometer operated with a 70 eV electron impact ionization method.

The column density of the deposited molecules, as well as products of energetic processing, were calculated from the infrared spectra using the formula

$$N = \int_{\text{band}} \frac{\tau}{A} d\nu, \quad (2)$$

where N is the column density in cm^{-2}, A is the band strength in cm· molecule^{-1}, and τ is the optical depth of the band. τ was determined from the absorption spectrum, using

$$\tau = \frac{\ln 10}{2} \cdot A_\nu \cdot \cos\varphi, \quad (3)$$

where ϕ is the angle of reflection ($\phi = 16^\circ$) and A_ν is the absorbance at IR photon energy ν.

The adopted band strengths of the ice compounds and the products of ice irradiation are listed in Table 1. The uncertainty of the column density of molecules determined by Equation (2) is mainly due to the effect of mixture on the band strengths and the overlapping between bands of different molecules in the mixture.

In the present work we focus the discussion on electron and thermal processing of H_2S–CH_3OH–NH_3–H_2O (the "with H_2S" ice mixture) and CH_3OH–NH_3–H_2O (the "without H_2S" ice mixture), expected for ice mixtures in KBOs and Trojans. The study of pure methanol ice was useful for the assignment of some bands in the "without H_2S" and the "with H_2S" mixtures and is also reported.

3. RESULTS

3.1. Electron Irradiation Initiated Chemistry

3.1.1. Pure Methanol Ice

Before studying the "with H_2S" and the "without H_2S" mixtures, examination of pure methanol ice (CH_3OH) was performed to aid in the interpretation of the more complicated mixtures. The irradiation of methanol ice has been reported previously for electrons (e.g., Bennett et al. 2007), ions (e.g., Moore et al. 1996), and UV photons (e.g., Gerakines et al. 1996). The column density of methanol in the deposited ice we estimated using Equation (2) to be 2.5×10^{18} molecules cm^{-2}. Taking a density of 1.020 g cm^{-3}

Table 1
Summary of Band Positions and Strengths Used in the Present Work

Molecule	Band	Band Strength	Reference	Comments
H_2O	1675	$4\ 10^{-18}$	Hudgins et al. (1993)	H_2O:CH_3OH:CO:NH_3 mixture
CH_3OH	1132	$3.2\ 10^{-18}$	Hudgins et al. (1993)	H_2O:CH_3OH:CO:NH_3 mixture
CH_3OH	1132	$1.8\ 10^{-18}$	Hudgins et al. (1993)	Pure CH_3OH
H_2S	2550	$2.9\ 10^{-17}$	Smith (1991)	Pure H_2S
NH_3	3367	$1.1\ 10^{-17}$	D'Hendecourt & Allamandola (1986)	Pure NH_3
CO_2	2339	$1.4\ 10^{-16}$	Hudgins et al. (1993)	Pure CO_2
CO	2134	$1.1\ 10^{-17}$	Gerakines et al. (1995)	Pure CO
OCS	2040	$1.5\ 10^{-16}$	Hudgins et al. (1993)	H_2O:OCS 2:1
OCN^-	2165	$1.3\ 10^{-16}$	Van Broekhuizen et al. (2004)	H_2O-NH_3–HNCO mixture
CH_4	1303	$4.7\ 10^{-18}$	Hudgins et al. (1993)	CH_4:H_2O mixture
H_2CO	1717	$9.6\ 10^{-18}$	Schutte et al. (1993)	Pure H_2CO

(Tauer & Lipscomb 1952) results in a calculated average thickness of 1.61 μm. This value is in agreement with the thickness of 1.7 μm estimated from the optical depth using the equation

$$d = \frac{\tau}{\left(\frac{4\pi k}{\lambda}\right)}, \quad (4)$$

where d is the average film thickness, τ is the optical depth, λ is the wavelength, and k is the imaginary optical index at λ. Equation (4) was applied using the same methanol band as for the column density calculations (1134 cm^{-1}) and $k = 0.081$ (Hudgins et al. 1993).

Figure 1 presents MIR spectra of CH_3OH before and after irradiation by 10 keV electrons with a fluence of 2×10^{21} eV cm^{-2}, which is the same fluence as was used to irradiate the more complex ice mixtures. New bands became apparent after irradiation and these products are summarized in Table 2.

We note a strong modification in the profile of the OH stretching band of methanol at 3260 cm^{-1} after irradiation. Palumbo et al. (1999) compared the profile of this methanol band after ion irradiation with the same band in a CH_3OH:H_2O ice mixture and suggested the production of water after methanol irradiation. This explanation was supported by a water band at 1651 cm^{-1} after irradiation. In addition to water, the electron irradiation chemistry of methanol ice leads to the formation of CO_2(2339 cm^{-1}), $^{13}CO_2$ (2273 cm^{-1}), CO (2134 cm^{-1}), H_2CO (1715 cm^{-1}), CH_4 (1302 cm^{-1}), and ethylene glycol $C_2H_4(OH)_2$ (1090, 885 and 861 cm^{-1}). These products are listed in Table 2 with the estimated values of the column densities and the N(compound)/$N$$CH_3OH$ production rate ratio for the main products. Hudson & Moore (1999) ruled out the assignment of the band at 1090 cm^{-1} to ethanol and assign it to ethylene glycol. One of the arguments used for this assignment is the straightforward mechanism explaining the formation of ethylene glycol, which consists of a radical–radical recombination reaction between two CH_2OH fragments. The band at 1715 cm^{-1} was assigned to H_2CO by Moore et al. (1996), while Gerakines et al. (1996) reported that methyl formate (H_3COHCO) also presents an infrared band in the same frequency. Because we do not observe the CH_3 rock mode of H_3COHCO at 1167 cm^{-1}, we assign the band at 1715 cm^{-1} to H_2CO. These products of solid-phase chemistry are in agreement with the photochemical and ion bombardment products reported in previous studies of methanol ice. A study of the reaction mechanisms following electron irradiation of methanol is reported by Bennett et al. (2007).

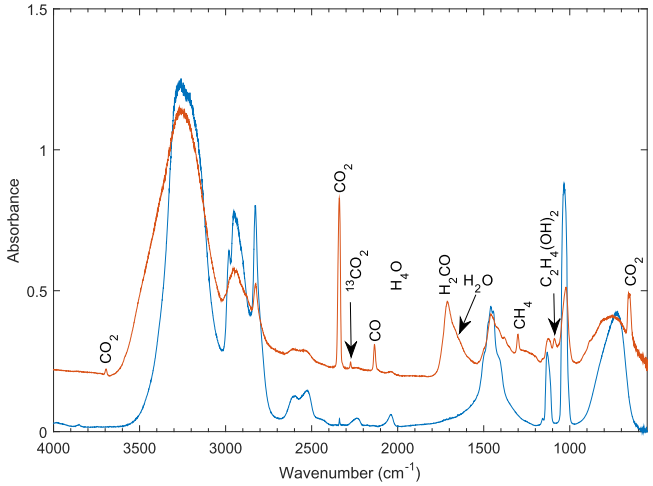

Figure 1. IR spectra of pure methanol deposited on a cold substrate (50 K) before (blue) and after (red) electron irradiation by a 10 keV electron beam (fluence = 2×10^{21} eV cm^{-2}).

Table 2
Infrared Band Assignments of Electron Irradiation of Methanol Ice. The Column Density of the Main Products is Estimated using Equation (2)

Band (cm^{-1})	Assignment	Column Density after Irradiation of CH_3OH (molecules cm^{-2})	N/N (CH_3OH)
2339	CO_2[a]	$2\ 10^{16}$	$8\ 10^{-3}$
2134	CO[a]	$1\ 10^{17}$	0.025
1717	H_2CO[a]	$4.5\ 10^{17}$	0.18
1651	H_2O[a]	…	…
1586	HCOOH[a]	…	…
1303	CH_4[a]	$2\ 10^{17}$	$8\ 10^{-2}$
1090, 885, 861	$C_2H_4(OH)_2$[b]	…	…

Notes. Band overlapping with methanol (no accurate column density can be obtained).
[a] Palumbo et al. (1999).
[b] Hudson & Moore (1999).

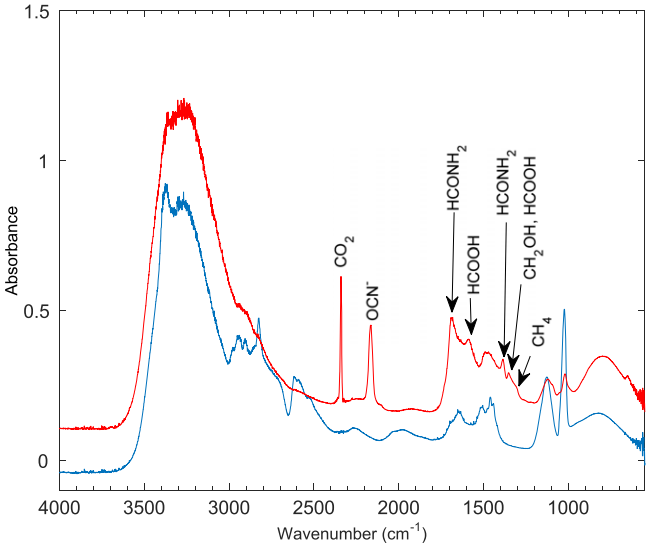

Figure 2. IR spectra of CH_3OH–NH_3–H_2O (2:2:1) deposited on a cold substrate (50 K) before (blue) and after (red) electron irradiation with 10 keV electron beam (fluence = 2×10^{21} eV cm^{-2}).

3.1.2. CH_3OH–NH_3–H_2O mixture (without H_2S)

Figure 2 presents MIR spectra of the CH_3OH–NH_3–H_2O (2:2:1) "without H_2S" mixture, both as deposited and after electron irradiation with a fluence of 2×10^{21} eV cm^{-2} at 50 K. Table 3 lists the infrared bands of the three components as well as their attribution according to the literature. The spectrum is dominated by methanol bands observed at 797, 1020, 1124, 1460, 2827, and 3250 cm^{-1}. The band at 3367 cm^{-1} is assigned to the ν_3 N–H stretching mode of ammonia. This band is shifted by about 8 cm^{-1} toward low energies compared to pure NH_3 ice (Holt et al. 2004). The same shift and broadening was observed for NH_3:H_2O ice compared with pure NH_3 ice by Moore et al. (2007b). Pure NH_3 ice also presents an intense band at 1070 cm^{-1}, which is assigned to ν_2 umbrella vibrations. This band is also broadened and shifted to 1109 cm^{-1} in the NH_3–H_2O ice where it overlaps with the intense band of CH_3OH centered at 1124 cm^{-1}. The ν_4 vibrational mode of NH_3 is observed at 1638 cm^{-1}, in agreement with the Moore et al. (2007b) spectrum of an NH_3–H_2O ice mixture. Estimated column densities for the three compounds of the mixture are $N(CH_3OH) = 3 \times 10^{18}$ molecules cm^{-2}, $N(NH_3) = 6 \times 10^{17}$ molecules cm^{-2}, and $N(H_2O) = 5 \times 10^{17}$ molecules cm^{-2}. We note that the ice is depleted in ammonia compared to gas mixture which can be explained by the lower sticking efficiency of NH_3 compared with H_2O and CH_3OH.

The red curve in Figure 2 shows the post-irradiation spectrum of the "without H_2S" mixture. We note a significant decrease of bands of initial reactive molecules (CH_3OH, NH_3, and H_2O) indicating that these molecules are partially consumed as the ice is irradiated. Bands appearing after irradiation are listed with their assignments in Table 3.

Among the new products we observed the same molecules produced by irradiation of pure methanol ice: CO_2, CO, CH_4, and H_2CO. The intense band at 2165 cm^{-1} in the "without H_2S" mixture is a common product from the processing of ices containing C, O, and NH_3 (Moore & Gerakines 2001). We assign this band to the cyanate anion (OCN^-). Reaction pathways proposed to explain the production of OCN^- involve CO (which was detected in our experiment) as reagent

Table 3
Assignment of Absorption Bands Observed in a "Without H_2S" Mixture (CH_3OH–NH_3–H_2O) Before and After Irradiation

	Band	Assignment
As deposited	797, 1020, 1124, 1460, 2827, 3250	CH_3OH[a]
	1638, 3367	NH_3[b]
	1655	H_2O[c]
Irradiation products	1717	H_2CO[a]
	2339	CO_2[a]
	2134	CO[a]
	1303	CH_4[a]
	1686, 1387	$HCONH_2$[d]
	2165	OCN^-[d]
	1589	HCOOH[e]

Notes.
[a] Palumbo et al. (1999).
[b] Holt et al. (2004).
[c] Moore et al. (2007b).
[d] Jheeta et al. (2013).
[e] Van Broekhuizen et al. (2004).

(Bockelée-Morvan et al. 2004; Pilling et al. 2010, and Jones et al. 2011). Proposed reaction pathways include

$$NH_3 \rightarrow NH_2 + H, \quad \text{(i)}$$

$$CO + NH_2 \rightarrow OCNH + H, \quad \text{(ii)}$$

$$CO + NH_2 \rightarrow OCNH_2, \quad \text{(iii)}$$

$$CO + NH \rightarrow OCNH, \quad \text{(iv)}$$

$$OCNH + NH_3 \rightarrow OCN^- + NH_4^+. \quad \text{(v)}$$

The main HNCO absorption at 2260 cm^{-1} (Lowenthal et al. 2002) is barely detectable in our experiment. This can be explained by the fact that HNCO reacts rapidly to give OCN^- as reported in Mispelaer et al. (2012).

Two intense bands appear at 1387 cm^{-1} and 1686 cm^{-1}. These bands were detected previously in ion (Moore & Gerakines 2001) and electron (Jheeta et al. 2013) irradiated CH_3OH–NH_3 ice and in a UV-irradiated H_2O–CO–NH_3 mixture (Van Broekhuizen et al. 2004). These studies assigned these bands to the biologically relevant molecule formamide ($HCONH_2$), which can be formed through a hydrogen addition to the $CONH_2$ radical produced from reaction (iii) above.

The column density of OCN^- after irradiation of the "without H_2S" mixture was estimated to be 4.7×10^{16} molecules cm^{-2} using the band at 2165 cm^{-1}. This corresponds to a production ratio $N(OCN^-)/N(NH_3) = 7.5\%$ and $N(OCN^-)/N(CH_3OH) = 0.8\%$ after irradiation with a 2×10^{21} eV cm^{-2} fluence.

3.1.3. H_2S–CH_3OH–NH_3–H_2O Mixture (with H_2S)

Figure 3 presents MIR spectra of the "with H_2S" mixture as deposited and after electron irradiation with a fluence of $\sim 2 \times 10^{21}$ eV cm^{-2} at $T = 50$ K. The most intense band of H_2S is located at 2556 cm^{-1} (Moore et al. 2007a). Pure methanol has a large band in the same region and the H_2S feature appears as a shoulder. We present a deconvolution between H_2S and methanol bands in Figure 4. Moreover the identification of H_2S is supported by the detection of this molecule within the volatiles desorbed from the "with H_2S" ice mixture (see Section 3.2 below). The proportions in the H_2S–CH_3OH–NH_3–H_2O mixture were 3:3:3:1 in the gas phase. However, the same proportions are

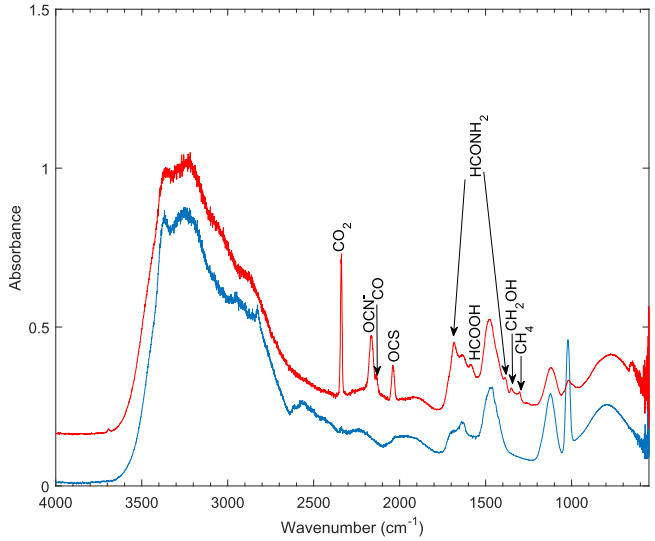

Figure 3. IR spectra of H_2S–CH_3OH–NH_3–H_2O (3:3:3:1) deposited on a cold substrate (50 K) before (blue) and after (red) electron irradiation with a 10 keV electron beam (fluence = 2×10^{21} eV cm^{-2}).

not guaranteed in the solid because the sticking coefficients of different species at 50 K are not necessarily the same. We estimated the proportions of each molecule in the solid phase by calculating the column density of each compound in the ice prior to irradiation. The determination of the integrated band areas for NH_3 and H_2S required a deconvolution of the absorption bands of these molecules from overlapping methanol bands (see Figure 4). The column densities for each species in the "with H_2S" mixture were: $N(H_2S) = 2 \times 10^{17}$ molecules cm^{-2}; $N(CH_3OH) = 10 \times 10^{17}$ molecules cm^{-2}; $N(NH_3) = 5 \times 10^{17}$ molecules cm^{-2}; $N(H_2O) = 12 \times 10^{17}$ molecules cm^{-2}. The composition of the ice as calculated from the respective column densities was estimated to be H_2S–CH_3OH–NH_3–H_2O = 7:35:17:41. We note that the ice is depleted in NH_3 and H_2S compared to the gas mixture. The diminution of the fractions of these two molecules can be due to their reaction to form NH_4SH in the deposited ice. The most intense band of NH_4SH and other ammonium salts that may be present is the NH_4^+ transition located at 1470 cm^{-1}. It is Unfortunate that this band overlaps with the methanol band in the same region and complicates the estimation of the column density of NH_4^+.

The red curve in Figure 3 shows the post-irradiation spectrum of the "with H_2S" mixture. We note a significant decrease in band intensity of the initial constituents, and particularly a total disappearance of the H_2S band. This is interpreted as complete destruction of the H_2S molecules by electron irradiation. Among products of irradiation we observe the same molecules produced after irradiation of the "without H_2S" mixture. Additionally, in the "with H_2S" mixture alone, after irradiation an intense band appears at 2040 cm^{-1}. This band is assigned to the C = O stretching mode of OCS, which is observed at 2019 cm^{-1} in pure OCS ice and shifted to 2046 cm^{-1} in OCS-H_2O and OCS-CO_2 mixtures (Ferrante et al. 2008). Previous experimental studies reported the formation of OCS after irradiation of ices containing CO or CO_2 as the carbon source and H_2S or SO_2 as sulfur source (Ferrante et al. 2008; Chen et al. 2015). Our assignment of the 2040 cm^{-1} band to OCS is supported by the absence of this band in the infrared spectrum of the irradiated "without H_2S" mixture, where no sulfur was present. OCS can be a product of reactions between a CO (which is produced from the dissociation of methanol as explained above) and an S atom or HS radical, as illustrated here:

$$H_2S \rightarrow H_2 + S, \quad \text{(vi)}$$

$$H_2S \rightarrow HS^{\cdot} + H, \quad \text{(vii)}$$

$$OC + S \rightarrow OCS, \quad \text{(viii)}$$

$$OC + HS^{\cdot} \rightarrow OCS + H. \quad \text{(ix)}$$

The column density of OCS after irradiation at 50 K (before heating) is 1.7×10^{16} molecules cm^{-2}. This corresponds to a ratio of $N(OCS)/N(H_2S) = 8.5\%$.

In Figure 3 it is noteworthy that the absorption band at 1477 cm^{-1} assigned to methanol is in the same position as the strong absorption band of (NH_4^+) (Howett et al. 2007). This

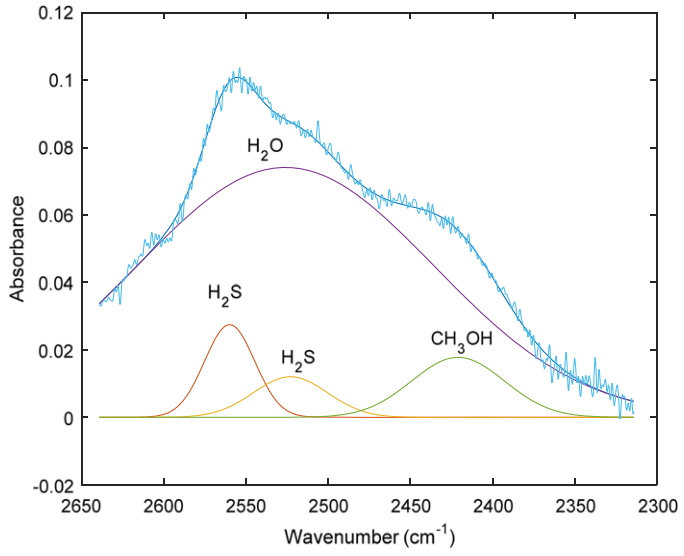

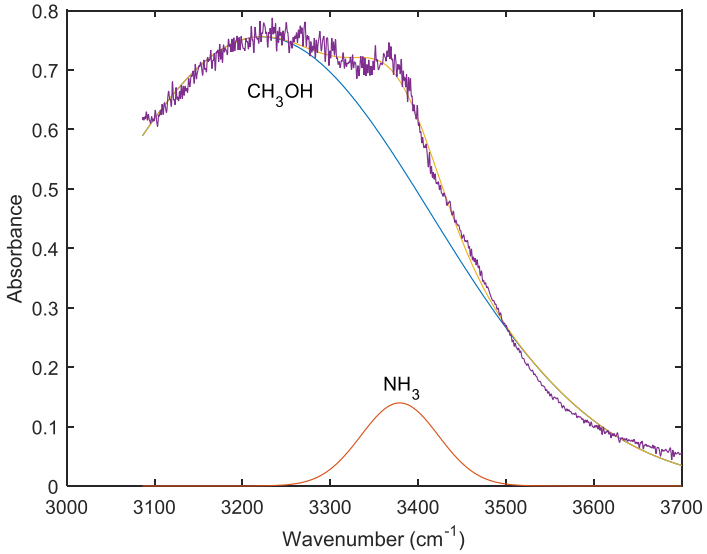

Figure 4. Left: Gaussian deconvolution for the 2556 cm^{-1} absorption corresponding to H_2S. Band A corresponds to CH_3OH, bands B and C correspond to H_2S (Jiménez-Escobar et al. 2014), and band D corresponds to H_2O. Right: Gaussian deconvolution for the 3367 cm^{-1} absorption corresponding to NH_3.

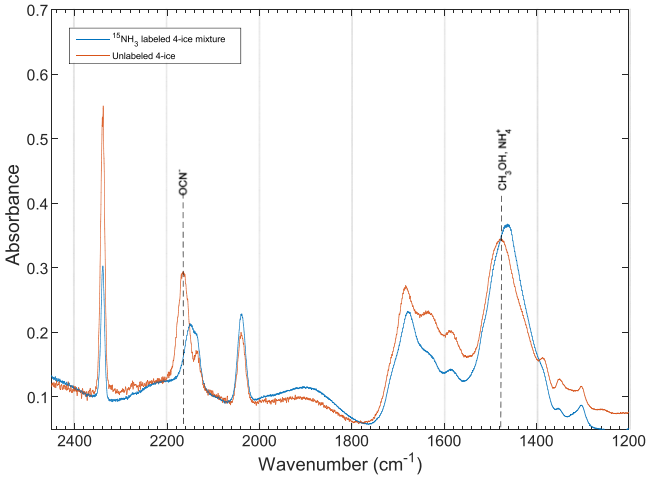

Figure 5. IR spectrum of irradiated "with H_2S" mixture (H_2S–CH_3OH–NH_3–H_2O) with $^{15}NH_3$ labeled ammonia compared with the unlabeled mixture.

makes it difficult to detect any production of the ammonium salt during the irradiation and heating of the sample. Thus, to assess the NH_4^+ chemistry, we have performed an irradiation experiment using ^{15}N labeled ammonia. Figure 5 compares the infrared spectra of labeled and unlabeled mixtures after irradiation. We observe a shift of 16 cm^{-1} of the OCN^- band in agreement with the isotopic shift 17 cm^{-1} measured in the matrix-isolated molecule (Maki & Decius 1959). This confirms our assignment of this band to OCN^-. More interestingly, we observe a shift by 10 cm^{-1} of the band at 1477 cm^{-1}. This shift is in agreement with the ^{15}N isotopic shift reported for the ammonium cation NH_4^+ (Morgan et al. 1957). The observed isotopic shift indicates that the absorption feature at 1477 cm^{-1} is not due only to the methanol; NH_4^+ also must contribute to this band. NH_4^+ is probably associated to OCN^- cation to form ammonium cyanate (Hudson et al. 2001). Ammonium hydrosulfide NH_4SH may also be present as result of co-depositing ammonia and hydrogen sulfide at 50 K Ammonium sulfide $(NH_4)_2SH$ and ammonium polysulfide $(NH_4)_2S_n$ may be produced by irradiation of NH_4SH. These compounds are proposed as the origin of the red, brown colors observed in Jupiter clouds (Taylor et al. 2004). The infrared absorption bands of these species are located between 300 and 700 cm^{-1}. Our spectra at this range lack sufficient signal-to-noise to confirm or deny the presence of these species.

3.2. Thermally Driven Chemistry

Figure 6 presents the infrared spectra of the irradiated "with H_2S" mixture at different temperatures (50, 100, 120, and 150 K) recorded during the heating of the sample at 0.5 minute^{-1} rate after the initial period of electron irradiation.

In these spectra we observed a new band appearing at 1257 cm^{-1} when the sample was warmed to 120 K, this band continued to grow while heating to 150 K. This band did not appear in the infrared spectra of the "without H_2S" mixture when heated to similar temperatures. The fact that this band is only observed in the S-containing mixture suggests that it is due to an S-containing molecule. We are not aware of published studies of ices containing both N- and S-bearing molecules, so band assignments here are provisional. We tentatively assign the 1257 cm^{-1} band to carbon monosulfide (CS). The CS molecule presents a single, intense band at 1270 cm^{-1} in the solid phase that has been assigned to the C–S stretching mode by Bohn et al. (1992) and by Bahou et al. (2000). The CS molecule was also observed at 1263 cm^{-1} as a product of CS_2 ice irradiation by Maity et al. (2013). The CS molecule can be formed from the reaction between C and S atoms, which are products of irradiation of CH_3OH and H_2S, respectively. These atoms are apparently not mobile at 50 K in the irradiated "with H_2S" mixture, but they become mobile and able to react at the relatively higher temperatures experienced during heating.

Based on labeled ammonia experiments, we are able to exclude the possibility that the band at 1257 cm^{-1} is attributed to the HNSO molecule. While this molecule presents an intense band at 1257 cm^{-1} in the gas phase and in an Ar matrix (Joo & Clouthier 1996), no change is observed when ^{15}N labeled ammonia is used in the mixture.

A second band also grew in intensity in the 120 K spectrum at 1586 cm^{-1}; this band is tentatively assigned to the carbon disulfide (CS_2) molecule. Pure CS_2 presents a large and intense band around 1550 cm^{-1} in the solid phase. Though different by

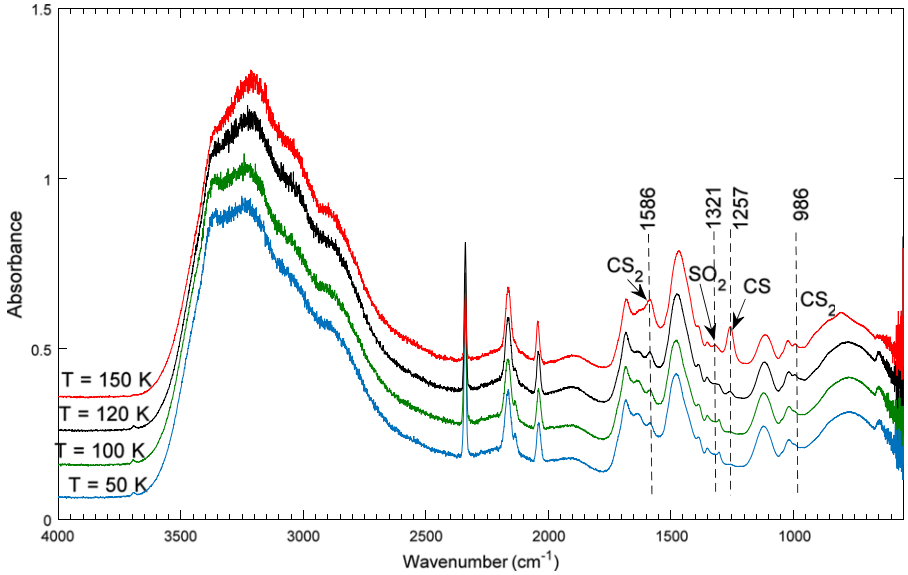

Figure 6. IR spectra of the "with H_2S" mixture irradiated at 50 K (blue) and then warmed to 100 K (green), 120 K (black), and 150 K (red).

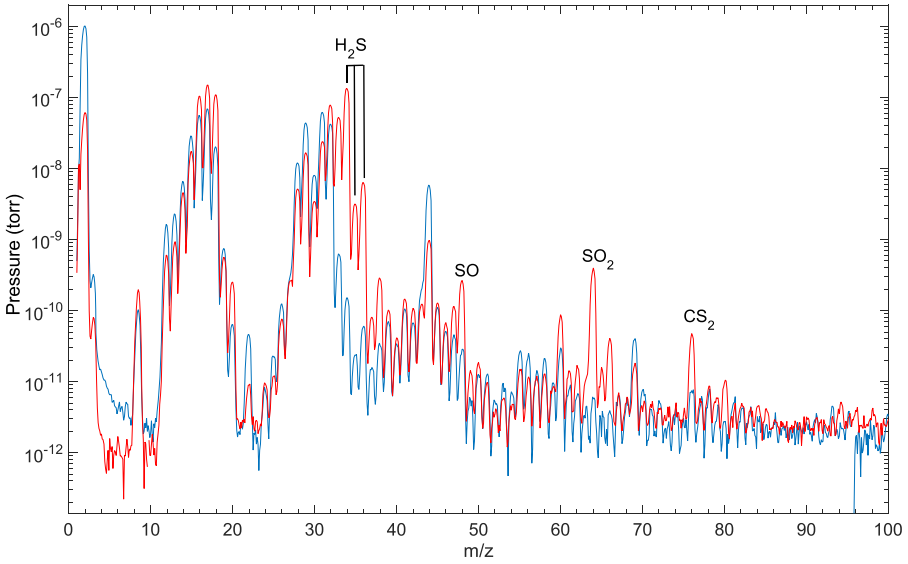

Figure 7. RGA mass spectrum recorded at 150 K for the irradiated "without H_2S" mixture (blue) and the "with H_2S" mixture (red).

several wavenumber, this assignment is supported by the observation of desorbed species appearing at 76 m/z, which corresponds to CS_2 and was observed only in the irradiated "with H_2S" experiment (see Figure 7). Jiménez-Escobar et al. (2014) reported the production of CS_2 after irradiation of CO–H_2S and CH_3OH–H_2S ices. We observe a new band appearing at 1321 cm^{-1} between 120 and 150 K. This band is assigned as sulfur dioxide (SO_2). Moore et al. (2007a) observed a strong band at 1325 cm^{-1} in pure SO_2 ice. The assignment here to an S-containing molecule is also supported by the fact that this band was totally absent in the IR spectra of the "without H_2S" mixture when warmed up to 150 K. Moreover, the assignment to an S-containing molecule is supported by the comparison of mass spectra at 150 K of the "without H_2S" and "with H_2S" mixtures (see Figure 7). In the "with H_2S" mixture we observe peaks at 64 m/z (SO_2) and 48 m/z (SO) that are not present for the "without H_2S" mixture. We observe also isotopic peak at 66 m/z due to $^{34}SO_2$ that support our detection of SO_2 in the mass spectrum.

4. DISCUSSION AND ASTROPHYSICAL APPLICATIONS

One hypothesis that aims to explain the red slope in the NIR spectra of KBOs and Trojans is the formation of an organic mantle on the surface of these bodies. Carbon-containing polymer products of irradiation of simple volatiles (e.g., methanol, methane) are suspected to be responsible for such a refractory crust. Theoretical treatments of the spectral properties of outer solar system objects take into account C and N containing organic weathering products. These studies typically use optical indices of Titan's and Triton tholins (C and N containing polymers) which have been extensively studied (e.g., Barucci et al. 2010). However, these models do not take into account the role that sulfur containing molecules can play on the color of TNO's.

Kuiper Belt objects and Jupiter Trojans are hypothesized to have a common primordial reservoir as suggested by dynamical models such as the Nice model (Morbidelli et al. 2005). The bimodality in colors within the populations of these two classes can be a result of the space weathering of primordial trans-Neptunian objects that have different surface chemical composition. In this context, Wong & Brown (2015, submitted) calculate that the sublimation line of H_2S split the common progenitor population of KBO's and Trojans into two groups: with and "without H_2S" in the surface. The authors conclude that this bimodality in the chemical composition could be the origin of the red and less-red two sub-populations within Jupiter Trojans.

In this work, we consider sulfur as an important component responsible for surface reddening, a hypothesis which is further supported by laboratory experiments reported in the literature that have shown that irradiated H_2S and H_2S–NH_3 ice mixtures result in a red slope in the NIR spectrum of ices (Lebofsky & Fegley 1976). We investigate here the role that hydrogen sulfide (H_2S) can play in the chemical alteration during the hypothetical migration of Jupiter Trojans from primordial trans-Neptunian region to their current position and chemical products produced during irradiation of plausible ice mixtures. Our experiments demonstrates that any initial H_2S present in the ice simulants is converted rapidly to chemical products (OCS, SO_2, CS, CS_2 and may be NH_4SH) upon irradiation. Electron irradiation was performed here in a matter of days at relatively high fluxes when compared with the outer solar system. Radiation fluences were scaled to the outer solar system based on the electron flux at 1 au, which was deduced from values given in (Bennett et al. 2013). We found that the total fluence received by our ice samples corresponds to a timescale of 0.2 Myr for an object at 5 au and 1.8 Myr at 15 au This indicates that space weathering reactions may occur on geologically short timescales for airless bodies whose surfaces consist of ices similar to those examined here.

Figure 8 presents the evolution of the integrated bands of the main irradiation products during the irradiation and heating of the "with H_2S" mixture. We note that the production of OCS molecules reaches a maximum after about 400 min of irradiation time and then stays almost constant during the irradiation phase of the experiment. This is probably explained by a rapid dissociation of the majority of the H_2S molecules within the first 400 minutes of the irradiation (corresponding to a fluence of 0.25×10^{21} eV cm^{-2}). The maximum value of OCS column density calculated using the integrated band at 2040 cm^{-1} was 1.7×10^{16} cm^{-2} (Table 4). In the experimental

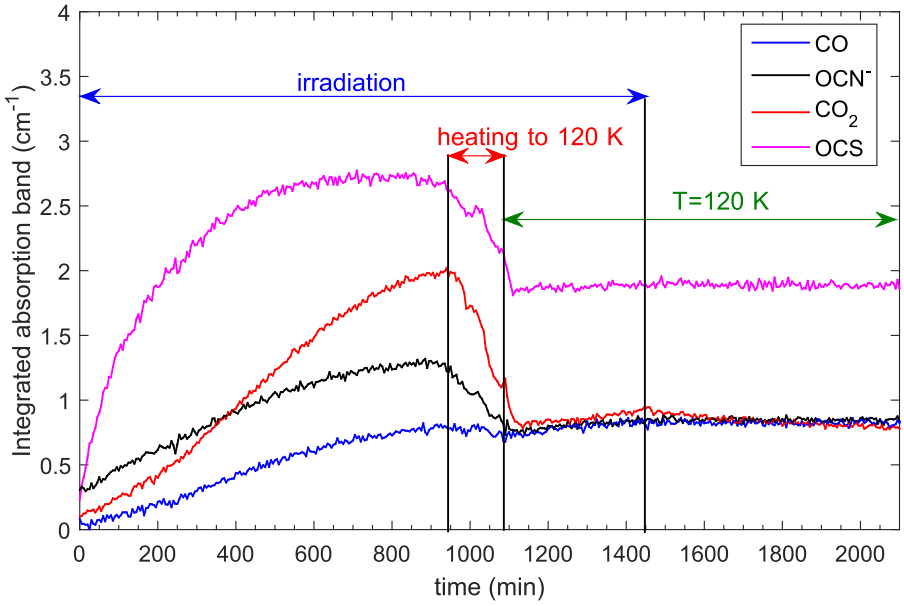

Figure 8. Evolution of integrated bands of OCS, OCN^-, CO, and CO_2 during irradiation and heating of the "with H_2S" mixture.

data presented in Figure 8, we irradiate the sample for 8 hr to test the stability of the irradiation products to heat and electron bombardment, mimicking the migration scenario of an icy object from the primordial tran-Neptunian disk to the Trojans' current position. About 70% of the initial amount of OCS remained after heating the system to 120 K while continuing electron irradiation. This amount remains stable during the test period where the temperature is fixed at 120 K for 16 hr. This indicates that OCS molecules might be produced in the icy surface of an outer solar system object that contains both methanol (CH_3OH) and hydrogen sulfide (H_2S) and is exposed to electron radiation and then remain.

To date, telescopic data have shown that thermal emissivity spectra of Trojans are featureless and dominated by absorption bands of silicate grains (Emery et al. 2006; Yang & Jewitt 2011). Direct searches for expected organic material signatures on the surfaces of Trojans have so far been unsuccessful, likely because of the low signal-to-noise ratio (S/N) obtained in this wavelength range. However, as telescopes become more sophisticated and potential missions to these bodies become more likely, new ways of detecting these organic signatures may become possible. The main outcome of this laboratory work is a prediction of detectable molecules and signatures that could serve as markers for objects that accreted beyond the stability line of H_2S and migrated to Jupiter current position. New observational approaches are, however, required to detect them. We propose to target molecules that help our understanding of the chemical composition of Jupiter Trojans by comparison with future high S/N telescopic data. According to the work herein, the detection of molecules like OCS (2050 cm^{-1}, 4.87 μm); CS_2 (1586 cm^{-1}, 6.3 μm) CS (1257, 7.9); and SO_2 (1325 cm^{-1}, 7.55 μm) may be a strong indication of the production of these molecules as results of irradiation and heating of H_2S containing icy surfaces. The link between detection of these molecules in red Trojans would be an argument that strengthens the hypothesis of the origin of red and less-red Jupiter Trojans as sulfurous and sulfurless primordial trans-Neptunian objects.

Table 4
Column Density of the Main Products of Irradiation of the "with H_2S" Mixture at 50 K and After Warming to 120 K

	Column density	
	After Irradiation at 50 K	After Irradiation and Warming to 120 K
OCS	$1.7\ 10^{16}$	$1.5\ 10^{16}$
CO_2	$3.87\ 10^{16}$	$2.06\ 10^{16}$
CO	$5.23\ 10^{16}$	$2.01\ 10^{16}$
OCN^-	$1\ 10^{16}$	$0.94\ 10^{16}$

5. CONCLUSION

This paper presents an experimental simulation of the chemical changes due to electron irradiation and heating of analogs of the outer solar system objects. We have particularly focused on the chemical differences due to radiation and thermal processing of ices with and "without H_2S". This molecule may be linked to objects formed inside and outside the stability line of H_2S, such as for primordial trans-Neptunian objects that migrated to the Jupiter Trojans' current positions (Wong & Brown 2015, submitted). Upon irradiation sulfur containing molecules (OCS, CS_2, SO_2, and CS) are formed only in the "with H_2S" mixture, containing H_2S. This sulfur chemistry that characterizes objects formed outside the stability line of H_2S could play an important role in the color of Jupiter Trojans. Produced molecules are stable in the irradiation and heating conditions, mimicking environment experienced by an object scattered from primordial KBO's reservoir region (beyond 15 au) to the current Jupiter orbit and indicating the persistence of observable products that testify to the initial presence of H_2S compounds over geologic time. This work identifies key target molecules and their absorption band positions that can be used to identify icy objects formed outside the sublimation line of H_2S and migrated to 5 au.

This work was conducted at the Jet Propulsion Laboratory, Caltech, under a contract with the National Aeronautics and Space Administration (NASA) and at the Caltech Division of

Geological and Planetary Sciences. This work was supported by the Keck Institute of Space Studies (KISS). Government sponsorship is acknowledged.

REFERENCES

Bahou, M., Lee, Y.-C., & Lee, Y.-P. 2000, JACS, 122, 661
Barucci, M. A., Ore, C. M. D., Alvarez-Candal, A., et al. 2010, ApJ, 140, 2095
Bennett, C. J., Chen, S. H., Sun, B.-J., Chang, A. H., & Kaiser, R. I. 2007, ApJ, 660, 1588
Bennett, C. J., Pirim, C., & Orlando, T. M. 2013, ChRv, 113, 9086
Bockelée-Morvan, D., Biver, N., Colom, P., et al. 2004, Icar, 167, 113
Bohn, R. B., Brabson, G. D., & Andrews, L. 1992, JPhCh, 96, 1582
Brunetto, R., Barucci, M. A., Dotto, E., & Strazzulla, G. 2006, ApJ, 644, 646
Chen, Y. J., Juang, K. J., Jimenez-Escobar, A., et al. 2015, ApJ, 798, 80
D'Hendecourt, L. B., & Allamandola, L. J. 1986, A&AS, 64, 453
Emery, J. P., Burr, D. M., & Cruikshank, D. P. 2011, AJ, 141, 25
Emery, J. P., Cruikshank, D. P., & Van Cleve, J. 2006, Icar, 182, 496
Ferrante, R. F., Moore, M. H., Spiliotis, M. M., & Hudson, R. L. 2008, ApJ, 684, 1210
Gerakines, P. A., Schutte, W. A., & Ehrenfreund, P. 1996, A&A, 312, 289
Gerakines, P. A., Schutte, W. A., Greenberg, J. M., & van Dishoeck, E. F. 1995, A&A, 296, 810
Hand, K. P., & Carlson, R. W. 2011, Icar, 215, 226
Holt, J. S., Sadoskas, D., & Christopher, J. P. 2004, JChPh, 120, 7153
Howett, C. J., Carlson, R. W., Irwin, R. P., & Calcutt, S. B. 2007, JOSAB, 24, 126
Hudgins, D. M., Sandford, S. A., Allamandolla, L. J., & Tielens, G. G. M. 1993, ApJS, 86, 713
Hudson, R. L., & Moore, M. H. 1999, Icar, 145, 661
Hudson, R. L., Moore, M. H., & Gerakines, P. A. 2001, ApJ, 550, 1140
Jheeta, S., Domaracka, A., Ptasinska, S., Sivaraman, B., & Mason, N. J. 2013, CPL, 556, 35
Jiménez-Escobar, A., Munoz Caro, G. M., & Chen, Y.-J. 2014, MNRAS, 443, 343
Jones, B. M., Bennett, C. J., & Kaiser, R. I. 2011, ApJ, 734, 78
Joo, L., & Clouthier, D. J. 1996, JChPh, 104, 8852
Lebofsky, L. A., & Fegley, M. B. 1976, Icar, 28, 379
Lowenthal, M. S., Khanna, R. K., & Moore, M. H. 2002, AcSpe, 58, 73
Maki, A., & Decius, J. C. 1959, Jchph, 31, 77
Maity, S., Kim, Y. S., Kaiser, R. I., et al. 2013, CPL, 213, 42
Marchis, F., Durech, J., & Castillo, J. 2012, AGUFM, P34A-07
Melita, M. D., Licandro, J., Jones, D. C., & Williams, I. P. 2008, Icar, 195, 686
Mispelaer, F., Theule, P., Duvernay, F., et al. 2012, A&A, 540, A40
Moore, H. M., & Gerakines, P. A. 2001, ApJ, 549, 52529
Moore, H. M., Hudson, R. L., & Carlson, R. W. 2007a, Icar, 189, 409
Moore, M. H., Ferrante, R. F., Hudson, R. L., & Stone, J. N. 2007b, Icar, 190, 260
Moore, M. H., Ferrante, R. F., & Nuth, J. A. 1996, P&SS, 44, 927
Morbidelli, A., Levison, H. F., Tsiganis, K., & Gomes, R. 2005, Natur, 435, 462
Morgan, H. W., Staats, P. A., & Goldstein, J. H. 1957, JChPh, 27, 1212
Nesvorný, D., Vokrouhlický, D., & Morbidelli, A. 2013, ApJ, 768, 45
Palumbo, M. E., Castorina, A. C., & Strazzulla, G. A. 1999, A&A, 342, 551
Pilling, S., Seperuelo Duarte, E., Domaracka, A., et al. 2010, A&A, 523, A7
Roig, F., Ribeiro, A. O., & Gil-Hutton, R. 2008, A&A, 483, 911
Schutte, W., Allamandola, L., & Sandford, S. 1993, Icar, 104, 1
Smith, R. G. 1991, MNRAS, 249, 172
Szabó, Gy. M., Ivezić, Ž, Jurić, M., & Lupton, R. 2007, MNRAS, 377, 1393
Tauer, K. J., & Lipscomb, Wm, N. 1952, Acta Cryst., 5, 606
Taylor, F. W., Atreya, S. K., Encrenaz, T. H., et al. 2004, in Jupiter: The Planet, Satellites and Magnetosphere, ed. F. Bagenal, T. E. Dowling, & W. McKinnon (Cambridge: Cambridge Univ. Press), 59
Thompson, W. R., Murray, B. G. J. P. T., & Khare, B. N. 1987, JGR, 92, 14933
Van Broekhuizen, F. A., Keane, J. V., & Schutte, W. A. 2004, A&A, 415, 425
Wong, I., & Brown, M. E. 2015, AJ, submitted
Wong, I., Brown, M. E., & Emery, J. P. 2014, AJ, 148, 11
Yang, B., & Jewitt, D. 2011, AJ, 141, 195